



CrossMark
click for updates

Cite this: *RSC Adv.*, 2016, 6, 108883

Enhanced photocatalytic activity on polarized ferroelectric KNbO_3 †

Qiang Fu,^{ab} Xianjie Wang,^{*a} Changyu Li,^c Yu Sui,^a Yaping Han,^b Zhe Lv,^a Bo Song^{ad} and Ping Xu^{*e}

In this paper, we demonstrate the enhanced photodegradation of rhodamine B on polarized ferroelectric KNbO_3 (KNO) particles. High-quality KNO samples were prepared using a solid-state reaction and polarized under different electric fields. The variation of XRD and piezoelectric coefficient (d_{33}) suggest an increased intensity of the ferroelectric polarization in the polarized samples. In contrast to the slow photodegradation rate of unpolarized KNO, the normalized photodegradation reaction rate constant was remarkably increased to 0.317 min^{-1} by the polarized KNO. The longer photoluminescence lifetime indicates that the enhancement of photocatalytic activity in polarized ferroelectric KNO powder is mainly attributed to the enhanced internal field. We believe this work may open up new avenues in photocatalysis using polarized ferroelectric materials.

Received 20th September 2016
Accepted 4th November 2016

DOI: 10.1039/c6ra23344a

www.rsc.org/advances

1. Introduction

The discharge of industrial effluent containing organic pollutants is becoming a serious challenge for society. Significant efforts, including filtration, sorption processes, biological treatment, and catalytic oxidation, are being made to remove these pollutants.^{1–6} Among the techniques that are being investigated, semiconductor photocatalysis is regarded as an effective way to degrade and remove hazardous pollutants from water. Electron–hole pairs can be generated in a semiconductor under light irradiation, and these are able to participate in redox reactions with pollutants. Several semiconductor systems have been investigated, but no satisfactory cost-effective approach has yet been found because some precious metals, such as Au and Ag, or their oxides must be added to enhance the photocatalytic activity.^{7–10}

Ferroelectric materials have spontaneous polarization arising from the displacement of the center of the positive and negative charges in a unit cell, and this could provide new possibilities for designing photovoltaic devices by promoting the separation of photo-excited carriers to a desirable extent.^{11–13}

Furthermore, ferroelectric polarization helps to inhibit the recombination of electrons and holes, just like p–n junctions of a typical photovoltaic or other diode structure. With a similar mechanism as that of p–n junctions, ferroelectric materials can also serve as new candidates for photocatalysis, and these have a significant influence on the surface photochemistry. For example, acceleration of the separation of electrons and holes by polarization in BaTiO_3 (BTO) bulk pellets has been demonstrated *via* the spatial selectivity of photo reduction and oxidation reactions.¹⁴ Cui *et al.* observed an enhanced photocatalytic activity in Ag-loaded BTO as a result of the influence of the ferroelectricity on the carrier separation.¹⁵ Recently, Su *et al.* prepared different-sized BTO nanoparticles (7.5 nm) with high monodispersity to investigate the effects of a ferroelectricity-enhanced photocatalytic reaction. These results clearly indicate that ferroelectricity can directly affect photocatalytic activity and that photocatalytic performance can be significantly increased by attaching Ag to the BTO surface.¹⁶ However, the relationship between polarization and photocatalytic reactions is not clear.

Recently, Density Functional Theory (DFT) and electronic structure analysis suggested that polarized ferroelectric oxide is a useful way to design an efficient photocatalyst.^{17,18} It is well known that the polarization of ferroelectrics can be reoriented by an applied electric field. KNbO_3 (KNO) is one of the most promising candidates for ferroelectric-based photovoltaic applications due to a higher Curie temperature (about $440 \text{ }^\circ\text{C}$).¹⁹ Much attention has been paid to morphological control and noble metal doping to improve the photocatalytic activity of KNO. Ag–KNO nanocomposites enhance the photocatalytic activity because the deposition of Ag nanoparticles results in continuous band gap states and increases electron density adjacent to the Fermi level.²⁰ Lan *et al.* observed an enhanced photocatalytic

^aDepartment of Physics, Harbin Institute of Technology, Harbin 150001, China. E-mail: wangxianjie@hit.edu.cn

^bDepartment of Physics, Northeast Forestry University, Harbin 150040, China

^cMaterial Science and Engineering College, Northeast Forestry University, Harbin 150040, China

^dAcademy of Fundamental and Interdisciplinary Sciences, Harbin Institute of Technology, Harbin 150001, China

^eSchool of Chemistry and Chemical Engineering, Harbin Institute of Technology, Harbin 150001, China. E-mail: pxu@hit.edu.cn

† Electronic supplementary information (ESI) available. See DOI: 10.1039/c6ra23344a

activity in one-dimensional KNO nanowires with Au nanoparticles due to surface plasmon resonance as well as interband transitions on Au nanoparticles.²¹ Zhang *et al.* found that orthorhombic KNO nanowires displayed RhB photodegradation about two-fold as large as their monoclinic counterparts.²² However, their photocatalytic efficiency was still very low.

In this paper, we investigated the influence of polarization on the photodegradation of rhodamine B (RhB) by KNO particles. High quality KNO samples were polarized under different electric fields, and variations of XRD and the piezoelectric coefficient (d_{33}) clearly suggested increased intensity of ferroelectric polarization. The photodegradation rate and photoluminescence lifetime were strongly increased after polarization, and this was mainly attributed to the enhanced internal field after polarization.

2. Experimental

2.1 Sample preparation

Stoichiometric powder with the composition of KNbO_3 (KNO) was prepared *via* the solid-state reaction technique, where the dried K_2CO_3 (99.5%) and Nb_2O_5 (99.9%) powders were used as raw materials. The raw materials were mixed and well-ground in absolute ethyl alcohol until it dried. The powder was then pressed into pellet disks and calcined at 900 °C for 24 h. The calcined mixture was then ground using an agate mortar and pressed into pellet disks 13 mm in diameter, and these were sintered at 1000 °C for 24 h surrounded by sacrificial powder of the same composition to inhibit volatilization of potassium. The prepared samples were polarized using a lab-made polarizing device. The system consists of two conductive needles, and the KNO pellet disk coated with palladium–silver paste on both sides was put in the middle for polarization. Three different polarized fields (5 kV cm^{-1} , 10 kV cm^{-1} , and 15 kV cm^{-1}) were used to polarize the KNO samples for 30 min. It is noted that the KNO pellet disk is destroyed if the polarizing field is higher than 20 kV cm^{-1} .

2.2 Characterization

The crystal structure of the KNO particles was characterized by X-ray diffraction (XRD, using the X'Pert XRD spectrometer with Ni-filtered Cu $K\alpha$ radiation, $\lambda = 1.5418 \text{ \AA}$) and X-ray photoelectron spectroscopy (XPS, ESCALAB 250Xi, Thermo Fisher Scientific). The dielectric properties of the samples were measured using the Agilent E4980A LCR meter. Ferroelectric data were collected with the Precision Premier II Ferroelectric Tester (Radiant Technology).

2.3 Photocatalysis

The photodegradation of rhodamine B (RhB) was assessed under UV light irradiation to evaluate the photocatalytic activity of the KNO samples. The concentration of the RhB solution was 10 mg L^{-1} , and 0.2 g of the KNO samples was used to degrade 200 ml of the RhB solution. Before light illumination, the suspension was magnetically stirred for 30 min in the dark to establish complete adsorption–desorption equilibrium. The

absorption spectra were collected using ultraviolet-visible (UV-vis) spectroscopy (TU-1901, Beijing Purkinje General). The photoluminescence (PL) lifetime was measured using a laser system with a wavelength of 375 nm and a frequency of 20 MHz (Becker and Hickl GmbH).

3. Results and discussion

Fig. 1a shows the XRD patterns of KNO samples at room temperature (RT), which can be indexed to a perovskite structure of pure KNO of an orthorhombic crystal system with the *Amm2* space group (JCPDS 71-0946).²³ The intensity of the (220) peak was higher than that of the (002) peak (Fig. 1b). The XPS spectra of K and Nb of the KNO samples are shown in Fig. S1.† The binding energy was determined by reference to the C 1s line. The binding energies of Nb 3d_{5/2} and Nb 3d_{3/2} are 206.7 eV and 209.4 eV, respectively, similar to the reported values of Nb⁵⁺.^{20,24} The binding energies of K 2p_{3/2} and K 2p_{1/2} are 291.3 eV and 294.1 eV, respectively, which confirms the existence of K⁺. Temperature-dependent dielectric constants at various frequencies (Fig. S2†) clearly show four phase transitions of KNO, and T_C is about 436 °C. The above results confirm the high quality of the as-obtained KNO samples.^{25,26}

Fig. 2 shows the *P*–*E* hysteresis loops of the polarized KNO samples at RT. It is clear that P_r of the KNO samples increases monotonically with the increase in the applied electric field, which is attributed to the fact that the ferroelectric domains can be switched easily at a higher applied electric field. The result verifies the existence of an internal electric field in KNO due to an intrinsic electric polarization.^{27,28}

The KNO samples were polarized using a lab-made polarizing device with three polarization fields (5 kV cm^{-1} , 10 kV cm^{-1} , and 15 kV cm^{-1}). The polarization intensity can be characterized from the ratio of $I(220)/I(002)$ from Fig. 1b. The relative intensities of (220)/(002) are 2.81, 2.74, and 3.03 after polarizing under 5, 10, and 15 kV cm^{-1} (1.40 for the non-polarized),

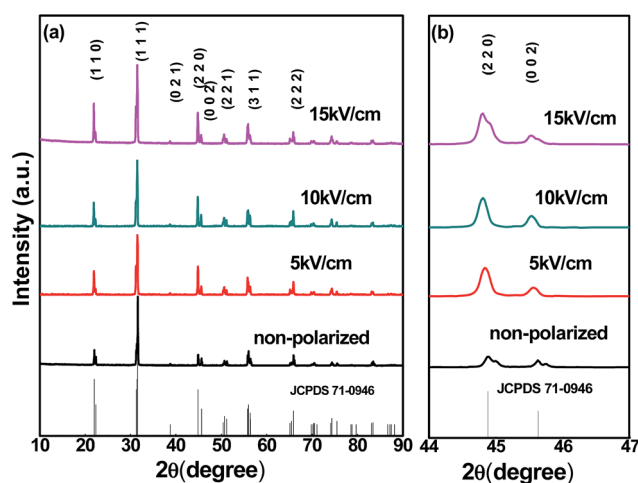


Fig. 1 (a) XRD patterns of non-polarized KNO and 5 kV cm^{-1} , 10 kV cm^{-1} , and 15 kV cm^{-1} polarized KNO samples. (b) The enlarged view of the (220) and (002) crystal planes.

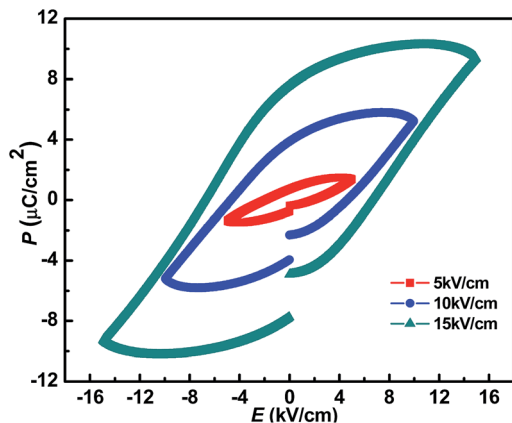


Fig. 2 P - E hysteresis loops of KNO polarized with different electric fields.

respectively, indicating more electric domains along the (220) crystal plane with increasing polarized fields.^{29,30} Furthermore, the alignment of electric domains enhances the separation of photogenerated electrons and holes, and thus the photocatalytic efficiency. As shown in Table S1,[†] the variation of lattice parameters calculated from XRD also suggest that the degree of polarization increases with stronger polarized electric field because the ferroelectric polarization of KNO arises from the displacement of the center of the positive and negative charges in a unit cell. The piezoelectric coefficient (d_{33}) is a useful parameter to confirm the ferroelectric polarization. The increased value of d_{33} also confirms the enhanced intensity of the ferroelectric polarization after being polarized (Table S1[†]).

It is well known that ferroelectric polarization helps to inhibit the recombination of holes and electrons that participate in redox reactions. Here, we find that the photodegradation rate can be strongly enhanced after polarization (Fig. 3). Only 40% RhB was degraded after 70 min of illumination using the non-polarized KNO. However, RhB will be completely degraded within 15 min using the polarized KNO samples. It has been generally assumed that the kinetics of photocatalytic decolorization of most organic compounds follows the Langmuir-Hinshelwood model:^{5,31,32}

$$r_i = -\frac{dC_i}{dt} = \frac{\kappa KC_i}{1 + \kappa KC_i} \quad (1)$$

where C_i is the molar concentration of the dye solution, κ is the reaction rate constant, and K is the adsorption coefficient of the dye to the catalyst. When C_i is small ($C_i < 10^{-3}$ M)³, $\kappa KC_i \ll 1$, and eqn (1) can be simplified to a pseudo-first-order equation:²⁰

$$r_i = -\frac{dC_i}{dt} = \kappa KC_i, \quad (2)$$

and eqn (2) can be given in the following relationship:

$$\ln \frac{C_0}{C} = \kappa_{\text{obs}} t \quad (3)$$

where C_0 is absorbance related to the initial concentration of the dye, and $\kappa_{\text{obs}} = \kappa K$ is the observed pseudo-first-order reaction rate constant. The fitted liner curves are shown in Fig. S3,[†]

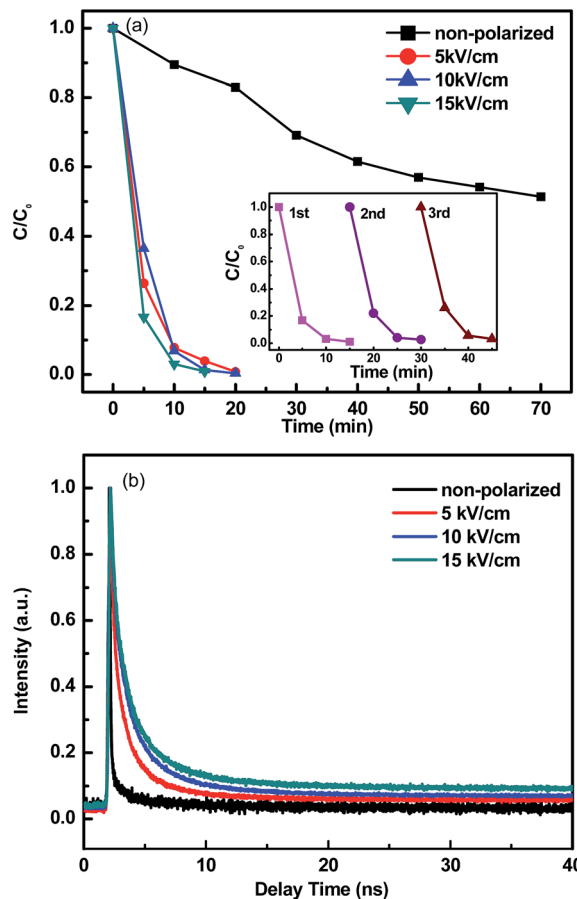


Fig. 3 (a) Photodegradation profiles of RhB under UV light irradiation, the inset shows the cycle stability of the 15 kV cm⁻¹ polarized KNO sample; (b) decay profiles of photoluminescence for non-polarized KNO and the polarized samples.

and the reaction rate, κ_{obs} , can be obtained from the fitted linear plot of $\ln(C_0/C)$ vs. t , which is shown in Table S2.[†] It is clear that the photodegradation rate of RhB increases from 0.010 min^{-1} to 0.317 min^{-1} with the increase of the polarized voltage.

Fig. S4[†] shows the UV-vis spectral changes of the RhB solutions in the presence of polarized KNO with a polarized voltage of 15 kV cm^{-1} and its corresponding successive colour change. The polarized KNO is very stable for the photodegradation of RhB (inset in Fig. 3a). It is well known that most of the ferroelectric photocatalysts used to degrade organic pollutants are made into nanostructures, and loaded with noble metal such as Ag, Au, and Pt, and thus synthetic processes are very complicated.^{7-10,16,28} Here, our samples are synthesized using a simple solid state reaction, and moreover, the degradation efficiency of the polarized KNO catalyst is markedly enhanced and the normalized photodegradation reaction rate constant was remarkably increased to 0.317 min^{-1} by the polarized KNO, which is much more effective than that of previous catalysts, such as Ag₂O-BTO hybrid nanocubes (about 2 h),³³ Ag-KNO nanocomposites (90 min),²⁰ and Ag-BTO hybrid nanocomposites (40 min).⁹ Therefore, our results clearly demonstrate that ferroelectric polarization is a useful way to enhance photocatalytic activity. In order to demonstrate the advantage of

polarization more directly, time-resolved photoluminescence (PL) lifetime was measured. As shown in Fig. 3b, the electrons excited from the polarized samples have a longer lifetime than that in the non-polarized one. This result clearly demonstrates that the internal field can inhibit the charge recombination, promoting the separation of the electrons and holes to enhance the photocatalytic activity.^{11,34,35}

The above results imply that the enhanced photocatalytic activity of polarized KNO samples may be interpreted from the enhanced internal electric field. Though there exists spontaneous polarization in non-polarized KNO, the intensity of the polarization is very limited because of the unordered ferroelectric domain. However, when an electric field was applied to polarize KNO, the ferroelectric domain in KNO tended to become ordered, and the polarization direction tended to point to the same direction. As shown in Fig. 4a, the spontaneous polarization with polarization vector P can be screened by free electrons and holes, respectively, and/or by ions or molecules adsorbed onto the surface from the solution forming a stern layer. The accumulation of free electrons on the surface (+) and holes on the surface (-) leads to downward and upward band bending, respectively. After the polarizing process, a permanent internal electric field was generated in KNO by the remanent polarization, as shown in Fig. 4b and c. When the polarized powder was irradiated with UV light, the electrons and holes were photo-generated and then separated by the internal electric field because of ferroelectric polarization, which led to the spatial separation of the oxidation and reduction reactions on opposite surfaces.¹⁵ Zhang *et al.* carried out control experiments with a number of scavengers to identify the major active species responsible for RhB degradation, and suggested that the $\cdot\text{OH}$ plays a more important role under UV than under visible-light.^{20,22} The photogenerated holes and electrons participated in

the formation of $\cdot\text{OH}$ and $\cdot\text{O}_2^-$, respectively. As shown in Fig. 4a, $\cdot\text{OH}$ was generated through the oxidation of OH^- and H_2O on the surface (-), and $\cdot\text{O}_2^-$ was formed from O_2 molecules through accepting electrons on the surface (+). Both $\cdot\text{OH}$ and $\cdot\text{O}_2^-$ can oxidize RhB and finally degrade it into H_2O , CO_2 , and other degradation products. Therefore, our results demonstrated clearly that the enhancement of photocatalysis activity in polarized ferroelectric powders can be mainly attributed to the enhanced internal field. Remanent polarization could assist in the increase of the photocatalytic activity in KNO.²⁸

4. Conclusion

In summary, this study shows that the photodegradation rate of RhB can be strongly increased through the polarization of ferroelectric KNO particles. Variations of the $I(220)/I(002)$ ratio in XRD and d_{33} confirm the increased intensity of ferroelectric polarization after polarizing the KNO samples. The longer PL lifetime reveals that the increased photocatalytic activity in polarized KNO particles can be mainly attributed to the enhanced internal field. Our results provide clear evidence that ferroelectric materials can act as promising photocatalysts in dye degradation and that polarization can greatly enhance the photocatalytic activity.

Acknowledgements

This work is supported by National Natural Science Foundation of China (No. 51472064, 51672057, 21671047), Science and Technology Innovation Talent Foundation of Harbin (2012RFXG110), and Program for Innovation Research of Science in Harbin Institute of Technology (PIRS of HIT 201616). Fundamental Research Funds for the Central University (Grant No. HIT-BRETHL.201220, HIT.NSRIF.2012045, HIT.ICRST.2010008), International Science & Technology Cooperation Program of China (2012DFR50020) and the Program for New Century Excellent Talents in University (NCET-13-0174).

Notes and references

- H. J. Yun, D. M. Lee, S. Yu, J. Yoon, H.-J. Park and J. Yi, *J. Mol. Catal. A: Chem.*, 2013, **378**, 221–226.
- Y. Kang, Y. Yang, L. C. Yin, X. Kang, G. Liu and H. M. Cheng, *Adv. Mater.*, 2015, **27**, 4572–4577.
- S. T. Ong, P. S. Keng, W. N. Lee, S. T. Ha and Y. T. Hung, *Water*, 2011, **3**, 157–176.
- H. Zhang, C. Wei, Y. Huang and J. Wang, *Ultrason. Sonochem.*, 2016, **30**, 61–69.
- I. K. Konstantinou and T. A. Albanis, *Appl. Catal., B*, 2004, **49**, 1–14.
- G. Liu, S. You, M. Ma, H. Huang and N. Ren, *Environ. Sci. Technol.*, 2016, **50**, 11218–11225.
- T. Som, G. V. Troppenz, R. R. Wendt, M. Wollgarten, J. Rappich, F. Emmerling and K. Rademann, *ChemSusChem*, 2014, **7**, 854–865.
- J. J. Chen, J. C. S. Wu, P. C. Wu and D. P. Tsai, *J. Phys. Chem. C*, 2012, **116**, 26535–26542.

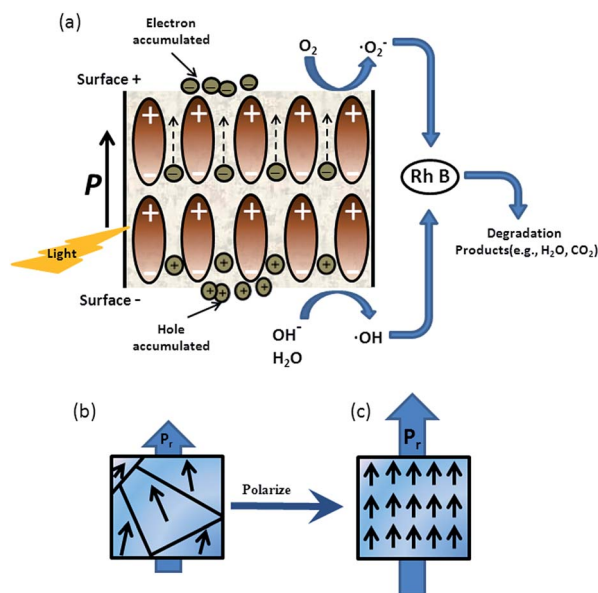


Fig. 4 (a) Schematic of photocatalysis with ferroelectric materials. The schematic of remanent polarization (P_r) of (b) non-polarized KNO and (c) polarized KNO samples.

- 9 N. T. Khoa, S. W. Kim, D. H. Yoo, S. Cho, E. J. Kim and S. H. Hahn, *ACS Appl. Mater. Interfaces*, 2015, **7**, 3524–3531.
- 10 S. Liu, C. Li, J. Yu and Q. Xiang, *CrystEngComm*, 2011, **13**, 2533–2541.
- 11 A. Kakekhani, S. Ismail-Beigi and E. I. Altman, *Surf. Sci.*, 2016, **650**, 302–316.
- 12 L. Li, P. A. Salvador and G. S. Rohrer, *Nanoscale*, 2014, **6**, 24–42.
- 13 L. Liang, X. Kang, Y. Sang and H. Liu, *Adv. Sci.*, 2016, **3**, 1500358.
- 14 J. L. Giocondi and G. S. Rohrer, *J. Phys. Chem. B*, 2001, **105**, 8275–8277.
- 15 Y. Cui, J. Briscoe and S. Dunn, *Chem. Mater.*, 2013, **25**, 4215–4223.
- 16 R. Su, Y. Shen, L. Li, D. Zhang, G. Yang, C. Gao and Y. Yang, *Small*, 2014, **11**, 202–207.
- 17 A. Kakekhani and S. Ismail-Beigi, *Phys. Chem. Chem. Phys.*, 2016, **18**, 19676–19695.
- 18 B. Modak and S. K. Ghosh, *RSC Adv.*, 2016, **6**, 9958–9966.
- 19 N. Yawata, H. Nagata and T. Takenaka, *Ferroelectrics*, 2014, **458**, 158–162.
- 20 T. Zhang, W. Lei, P. Liu, J. A. Rodriguez, J. Yu, Y. Qi, G. Liu and M. Liu, *J. Phys. Chem. C*, 2016, **120**, 2777–2786.
- 21 J. Lan, X. Zhou, G. Liu, J. Yu, J. Zhang, L. Zhi and G. Nie, *Nanoscale*, 2011, **3**, 5161–5167.
- 22 T. Zhang, W. Lei, P. Liu, J. A. Rodriguez, J. Yu, Y. Qi, G. Liu and M. Liu, *Chem. Sci.*, 2015, **6**, 4118–4123.
- 23 H. Du, W. Zhou, F. Luo, D. Zhu, S. Qu and Z. Pei, *Appl. Phys. Lett.*, 2007, **91**, 182909.
- 24 R. Wang, Y. Zhu, Y. Qiu, C.-F. Leung, J. He, G. Liu and T.-C. Lau, *Chem. Eng. J.*, 2013, **226**, 123–130.
- 25 B. Sundarakannan, K. Kakimoto and H. Ohsato, *J. Appl. Phys.*, 2003, **94**, 5182–5187.
- 26 G. Shirane, R. Newnham and R. Pepinsky, *Phys. Rev.*, 1954, **96**, 581–588.
- 27 P. A. Markovin, V. V. Lemanov, M. E. Guzhva, P. P. Syrnikov and T. A. Shaplygina, *Phys. Solid State*, 2014, **56**, 989–995.
- 28 S. Park, C. W. Lee, M.-G. Kang, S. Kim, H. J. Kim, J. E. Kwon, S. Y. Park, C.-Y. Kang, K. S. Hong and K. T. Nam, *Phys. Chem. Chem. Phys.*, 2014, **16**, 10408–10413.
- 29 S. Li, A. S. Bhalla, R. E. Newnham, L. E. Cross and C. Y. Huang, *J. Mater. Sci.*, 1994, **29**, 1290–1294.
- 30 T. Takaaki, K. Yutaka, O. Naoki, T. Tadashi and F. Osamu, *Jpn. J. Appl. Phys., Part 1*, 1997, **36**, 5970.
- 31 W. Baran, E. Adamek and A. Makowski, *Chem. Eng. J.*, 2008, **145**, 242–248.
- 32 J.-M. Herrmann, *Catal. Today*, 1999, **53**, 115–129.
- 33 H. Li, Y. Sang, S. Chang, X. Huang, Y. Zhang, R. Yang, H. Jiang, H. Liu and Z. L. Wang, *Nano Lett.*, 2015, **15**, 2372–2379.
- 34 H. Yu, X. Wang, W. Hao and L. Li, *RSC Adv.*, 2015, **5**, 72410–72415.
- 35 H. Lee, K. Heo, J. Park, Y. Park, S. Noh, K. S. Kim, C. Lee, B. H. Hong, J. Jian and S. Hong, *J. Mater. Chem.*, 2012, **22**, 8372–8376.